

## Computational Study of Highly Efficient SnO<sub>2</sub> ETL-based Inorganic Perovskite Solar Cell

**Abstract.** The growing demand for high Power Conversion Efficiency (PCE) in Perovskite Solar Cells (PSCs) has increased the need for the introduction of new material combinations. The conventional TiO<sub>2</sub> Electron Transport Layer (ETL) has reached its maturity limit, and no further progress can be made. Therefore, the replacement with the SnO<sub>2</sub> layer is seen as very reasonable. Furthermore, the crystallization of TiO<sub>2</sub> requires a high-temperature annealing process, thus obliterating its use in flexible applications, and increasing fabrication costs. This study numerically elaborated on the potential of SnO<sub>2</sub> as an ETL in PSCs using the Solar Cell Capacitance Simulator (SCAPS-1D). The combination of SnO<sub>2</sub> ETL with solid-state CUSCN HTL is also deliberated to provide an alternative to the use of all inorganic PSCs, where the cell consists of ITO/ SnO<sub>2</sub> /CH<sub>3</sub>NH<sub>3</sub>PbI<sub>3</sub>/CuSCN/Au. Numerous key parameters of SnO<sub>2</sub> have influenced cell performance, including operating temperature, layer thickness, dopant density and defect density state. The highest PCE has been recorded reaching up to 24.14% with FF of 85.99%, VOC of 1.15V, and JSC of 24.42 mA/ cm<sup>2</sup> from the optimized cell structure. However, it can be seen that the impact of high defect density has had a profound effect on PCE performance, thus illuminating the comprehensive concern required in containment. This may provide a guideline prior to the future fabrication of PSCs utilizing the SnO<sub>2</sub> as ETL.

**Streszczenie.** Rosnące zapotrzebowanie na wysoką wydajność konwersji energii (PCE) w perowskitowych ogniwach słonecznych (PSC) zwiększyło potrzebę wprowadzenia nowych kombinacji materiałów. Konwencjonalna warstwa transportu elektronów TiO<sub>2</sub> (ETL) osiągnęła swój limit dojrzałości i nie można poczynić dalszych postępów. Dlatego też zastąpienie warstwą SnO<sub>2</sub> wydaje się bardzo rozsądne. Co więcej, krystalizacja TiO<sub>2</sub> wymaga procesu wyżarzania w wysokiej temperaturze, co eliminuje jego zastosowanie w elastycznych zastosowaniach i zwiększa koszty produkcji. W tym badaniu opracowano numerycznie potencjał SnO<sub>2</sub> jako ETL w PSC przy użyciu symulatora pojemności ogniw słonecznych (SCAPS-1D). Rozważa się również połączenie SnO<sub>2</sub> ETL z półprzewodnikowym CUSCN HTL, aby zapewnić alternatywę dla stosowania wszystkich nieorganicznych PSC, gdzie ogniwo składa się z ITO/SnO<sub>2</sub>/CH<sub>3</sub>NH<sub>3</sub>PbI<sub>3</sub>/CuSCN/Au. Na wydajność ogniwa wpływa wiele kluczowych parametrów SnO<sub>2</sub>, w tym temperatura robocza, grubość warstwy, gęstość domieszki i stan gęstości defektów. Odnotowano najwyższy współczynnik PCE sięgający 24,14%, przy FF wynoszącym 85,99%, VOC wynoszącym 1,15 V i JSC wynoszącym 24,42 mA/cm<sup>2</sup> ze zoptymalizowanej struktury komórkowej. Można jednak zauważyć, że wpływ dużej gęstości defektów miał głęboki wpływ na wydajność PCE, rzucając w ten sposób światło na wszechstronną troskę wymaganą w zakresie powstrzymywania. Może to stanowić wytyczne przed przyszłym wytwarzaniem PSC wykorzystujących SnO<sub>2</sub> jako ETL. (Badanie obliczeniowe wysoce wydajnej nieorganicznej ogniwa słonecznego z perowskitu na bazie SnO<sub>2</sub> ETL)

**Keywords:** SnO<sub>2</sub>, perovskite solar cell, SCAPS-1D, ETL.

**Słowa kluczowe:** SnO<sub>2</sub>, perowskitowe ogniwo słoneczne, SCAPS-1D, ETL.

### Introduction

Perovskite Solar Cell (PSC) is an emerging solar cell with excessive progress in the last two decades, making it a promising candidate as a future energy source [1]. Perovskite was discovered in 2009 and named after Lev Perovski, who discovered it as the third generation of solar cell technology. Typically, PSC has three important layers, which are the ETL (SnO<sub>2</sub>), the HTL (CuSCN), and the absorber layer (Perovskite). These three layers are sandwiched with each other to produce a solar panel [2], [3].

ETL material is one of the most significant aspects of a solar cell. It plays a crucial role in extracting and transporting photogenerated electron carriers and serves as a hole-blocking layer by suppressing charge recombination [4]. TiO<sub>2</sub> has been widely used as an ETL in PSC. However, it is not very efficient for charge extraction at the interface, especially in planar structures [5], [6]. Meanwhile, other ETL materials such as SiO<sub>2</sub>, ZrO<sub>2</sub>, SnO<sub>2</sub>, and ZnO have been suggested to overcome the limitations of TiO<sub>2</sub>. According to the research that has been conducted, SnO<sub>2</sub> has stood out the most compared to the others. It has excellent chemical stability, U-V resistance, high charge extraction, and greater band alignment than other ETLs [7], [8].

SnO<sub>2</sub> material is chosen as the ETL in this project because of its favourable advantages. A wide bandgap that SnO<sub>2</sub> has is higher than other ETL materials, allowing it to have a superior light transmittance of 90% in glass [9], [10]. It enables SnO<sub>2</sub> to absorb less UV light while offering better device stability. Other than that, it has up to 240 cm<sup>2</sup> (Vs)<sup>-1</sup> mobility of electrons, which is considered 100 times higher than TiO<sub>2</sub> [9], [11]. High electron mobility helps it to extract

electrons efficiently. SnO<sub>2</sub> is easily processed at low temperatures, making it suitable for flexible solar cells and tandem solar cells [11].

Maciej Łuszczek et al., used SCAPS-1D software to simulate their analysis on perovskite solar cells with three different ETLs, which are TiO<sub>2</sub>, SnO<sub>2</sub>, and ZnO. In this study, SnO<sub>2</sub> has the best performance and the highest PCE compared to the other ETLs. This is due to certain attributes that SnO<sub>2</sub> owns, such as better band alignment and stability under ultraviolet illumination [12]. The PCE achieved is 17.08%, 18.33%, and 17.53% by TiO<sub>2</sub>, SnO<sub>2</sub>, and ZnO, respectively.

The electron mobility of SnO<sub>2</sub> was also investigated by Peng Zhao et al., [13]. They claim that the device performs optimal performance with a PCE of 20.43% when the SnO<sub>2</sub> electron mobility goes beyond 10<sup>-3</sup> cm<sup>2</sup>.(Vs)<sup>-1</sup>[13]. They reported that when the electron mobility is less than 10<sup>-4</sup> cm<sup>2</sup>.(Vs)<sup>-1</sup>, the recombination rate increases and causes the JSC and FF to decrease. The overall PCE has been obtained with an efficiency of 20.43%, JSC 21.5 mA/ cm<sup>2</sup>, and 81.12% FF.

Another simulation analysis is conducted by Yassine Raoui et al., where the perovskite performance is observed by using different ETL and HTL layers. The final results concluded that SnO<sub>2</sub> achieved the highest PCE compared to the other ETL (TiO<sub>2</sub> and ZnO). The device is structured as FTO/ETL/MAPbI<sub>3</sub>/Spiro-OMeTAD/Au [14]. The thickness of the ETL layers is equal to 90nm. SnO<sub>2</sub> demonstrated greater current density due to the increased light absorption by the perovskite layer, which is also reflected in the External Quantum Efficiency (EQE) rise in the 300 – 450 nm spectral range [14]. Raoui et al., also found that the

increases in the thickness of ETL lead to attenuation of  $V_{OC}$ ,  $J_{SC}$ , and  $P_{CE}$  of both  $TiO_2$  and  $ZnO$ . On the contrary, the  $SnO_2$  performance parameter has no obvious variations in its value.

Later, in 2020, Elham and Seyed analyzed the performance of  $SnO_2$  on perovskite solar cells using SCAPS-1D and AMPS simulation software. It was analyzed with the  $FTO/SnO_2/CH_3NH_3PbI_3/NiO/Au$  structure. The optimum thickness of  $SnO_2$  and its electron density concentration is 140nm to 160 nm and  $10^{18} \text{ cm}^{-3}$ , respectively [15]. It also stated that the  $V_{OC}$  is reduced in this research when the operating temperature increased from 300K to 440K. This is due to the temperature's dependency on the reverse saturation current.

Furthermore, when the bandgap energy was decreased to some amount, the recombination between the valence band and the conduction band was improved. The majority of free electrons are generated in the conduction band energy, but high temperatures can cause the recombination of holes and electrons, making the bandgap energy unstable [16]. As a result,  $J_{SC}$  is decreasing. The drop in  $V_{OC}$  and  $J_{SC}$  concentrations caused by the increase in working temperature results in a loss in performance.

### Methodology - Device simulation

In this study, the PSC device modelling framework comprises five layers. The layers included ITO as the front contact,  $CH_3NH_3PbI_3$  (an absorber),  $SnO_2$  and  $CuSCN$  as an ETL and HTL, respectively, and Gold (Au) as the back contact (Fig. 1). The PSC efficiency has been optimized by considering a few characteristics focused on  $SnO_2$ . For example,  $SnO_2$  thickness,  $SnO_2$  doping density, the

operating temperature of photovoltaic cells, and a defect interface are some of the factors listed. The first step of the analysis is carried out by performing a numerical simulation on SCAPS-1D software. The parameter of each structured layer is studied and optimized to achieve the best efficiency. In this simulation, the solar cell's efficiency value (PCE), open-circuit voltage ( $V_{OC}$ ), short circuit current ( $J_{SC}$ ), and fill factor (FF) were considered to be recorded and studied from the J-V curve obtained.

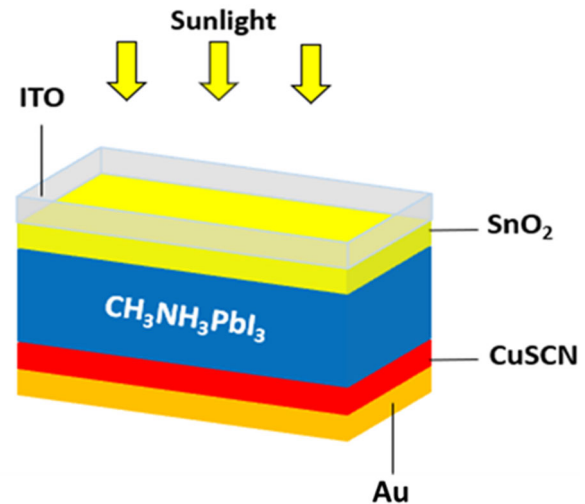


Fig. 1. The structure of PSC for simulation analysis

Table 1. Input parameter of numerical analysis for PSC structure

Layer	CuSCN [17]	ITO[18]	$SnO_2$ [17]	$CH_3NH_3PbI_3$ [17]
Layer thickness, d ( $\mu\text{m}$ )	350	200	Varied	600
Bandgap energy, $E_g$ (eV)	3.4	3.6	3.6	1.55
Electron affinity, (eV)	2.1	4.1	4	3.93
Dielectric permittivity, $\epsilon$ (relative)	10	10	9	30
Effective density of conduction band, $N_c$ ( $\text{cm}^{-3}$ )	$2.2 \times 10^{21}$	$2 \times 10^{18}$	$2.2 \times 10^{18}$	$2.2 \times 10^{18}$
Effective density of valence band, $N_v$ ( $\text{cm}^{-3}$ )	$1.8 \times 10^{21}$	$1.8 \times 10^{19}$	$1.8 \times 10^{19}$	$1.8 \times 10^{19}$
Thermal velocity of electrons, $V_e$ ( $\text{cm s}^{-1}$ )	100	0.001	100	2
Thermal velocity of holes, $V_h$ ( $\text{cm s}^{-1}$ )	25	0.1	25	2
Electron mobility, $\mu_e$ ( $\text{cm}^2/V_s$ )	$1 \times 10^7$	$1 \times 10^7$	$1 \times 10^7$	$1 \times 10^7$
Hole mobility, $\mu_h$ ( $\text{cm}^2/V_s$ )	$1 \times 10^7$	$1 \times 10^7$	$1 \times 10^7$	$1 \times 10^7$
Density of donors, $N_D$ ( $\text{cm}^{-3}$ )	NA	$1 \times 10^{19}$	Varied	NA

### Analysis of working temperature

Working temperature is one of the critical aspects that can greatly impact the photovoltaic performance of the PSCs. In this simulation, the temperature values varied are in a range of 300 K to 500 K with steps of 20 K. The graph shows a downward trend in efficiency as the operating temperature rises with an inclination of  $-0.0417 \text{ \%}/\text{K}$ , as shown in Fig. 2. All the parameters except  $J_{SC}$  decline monotonically as the temperature rises, except for a very slight increase in  $J_{SC}$  value. This is due to the fact that the material's carrier concentration, charge mobility, resistance, and bandgap will all be significantly impacted by higher temperatures, resulting in a shift in the PV's key properties [16][19]. In addition, the increased carrier concentration in the semiconductor is generated by a higher operating temperature, particularly the rate of internal carrier recombination.  $V_{OC}$  decreases as a result of a rise in reverse saturation current

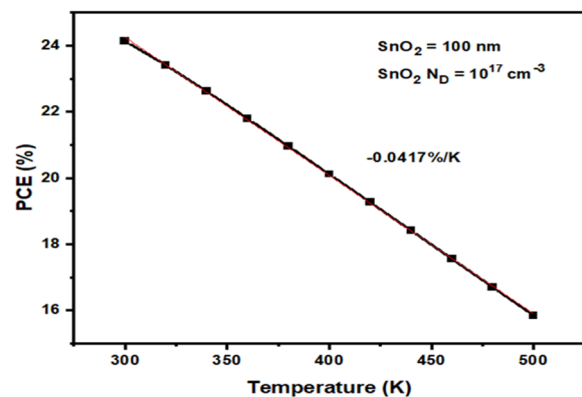


Fig. 2. The analysis of efficiency is based on the variation of working temperature.

### Analysis of the variation of SnO2 thickness

The thickness analysis for ETL SnO<sub>2</sub> is performed by altering the layer thicknesses in the same structure. For this study, only the ETL layers are altered for each simulation. The thickness of SnO<sub>2</sub> is varied from 0.005 μm to 1 μm. The P<sub>CE</sub> is affected by the increasing thickness of ETL (Fig. 3). It causes attenuation of P<sub>CE</sub>. It also reduces the cell's current and voltage, but the value is insignificant. The P<sub>CE</sub> constantly decreased until, at a thickness of 0.20 μm, the P<sub>CE</sub> stopped to decrease, this may be because it has reached the minimum efficiency. The attenuation of P<sub>CE</sub> due to a thick ETL can have a multitude of impacts. For example, the thicker the ETL may result in the distance for the electron to reach ITO, which is farther and raises the device's series resistance and lowers the fill factor, resulting in the efficiency of the solar cells dropping [20], [21].

Moreover, the electron may tend to enhance the recombination rate and reduce the V<sub>OC</sub>. According to Xiong et al., [20], highly efficient PSCs have a preference for thin compact layers. It is plausible to believe that a thin compact layer can facilitate electron extraction and reduce charge carrier combination due to its short diffusion length [20]. This is why a thinner ETL is preferable, where more photons can pass through the ETL layer into the absorber layer and be absorbed there. The thickness of 0.5 μm has the highest P<sub>CE</sub>, which is 25.83%. However, it is not a suitable thickness for the fabrication process. Therefore, in this analysis, the thickness of 0.1 μm is selected as an optimum thickness with a P<sub>CE</sub> of 24.14%.

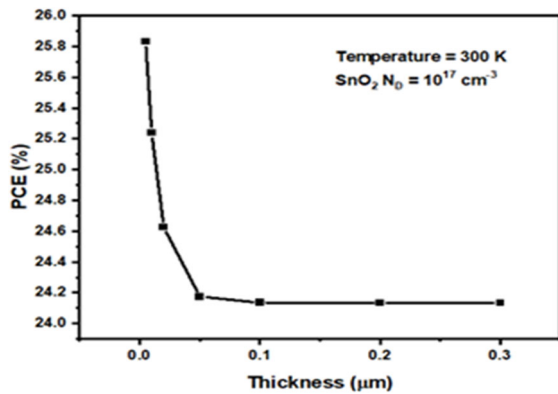


Fig. 3. The analysis of efficiency is based on the variation of SnO<sub>2</sub> thickness.

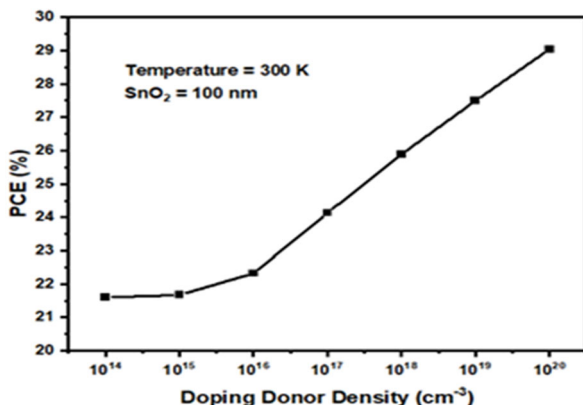


Fig. 4. The analysis of efficiency based on the variation of doping donor density.

### Analysis of the variation of doping donor density

Next, the analysis of doping donor density varied from 10<sup>15</sup> cm<sup>-3</sup> to 10<sup>20</sup> cm<sup>-3</sup>. The efficiency rises with doping donor density (Fig. 4). Increasing doping is equivalent to increasing the number of impurities in the semiconductor to

modulate its electrical, optical, and structural properties [19][22]. Therefore, as the amount of impurity in the semiconductor increases, more free charge will be created in the semiconductor. When the free charge increases, it indicates that there is more current flowing through the system at once, causing the series resistance to fall [23]. As a result, efficiency has been boosted. The optimum doping donor density obtained is 10<sup>17</sup> cm<sup>-3</sup>. As for the FF, it is greatly affected by the increase in doping density. The FF increased drastically from 10<sup>15</sup> to 10<sup>18</sup> cm<sup>-3</sup>, gradually increasing as doping exceeded 10<sup>18</sup>.

### Analysis of the variation of doping acceptor density

Following that, the analysis of doping acceptor density of CuSCN is varied from 10<sup>14</sup> cm<sup>-3</sup> to 10<sup>20</sup> cm<sup>-3</sup>. The graph illustrates the efficiency of the device increase as the doping acceptor density increase (Fig. 5). Increasing doping is comparable to increasing the number of impurities in the semiconductor to vary its electrical, optical, and structural properties [18][24]. Doping SnO<sub>2</sub> can boost its characteristics, hence improving the performance of PSCs [20]. Therefore, when the amount of impurity in the semiconductor grows, more free charge will be produced in the semiconductor. When the free charge increases, it implies that more current flows through the system at once, causing the series resistance to falls. As a result, the efficiency has been enhanced.

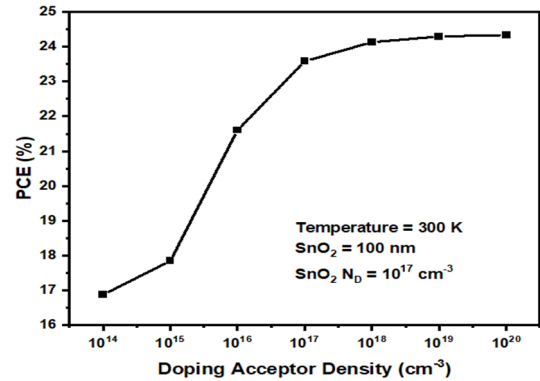


Fig. 5. The analysis of efficiency based on the variation of doping acceptor density.

The variation of recombination rate is analyzed with two types of recombination rates. The first one is the recombination rate of the defect density at the interface of SnO<sub>2</sub> and CH<sub>3</sub>NH<sub>3</sub>PbI<sub>3</sub> layers. This analysis aims to observe the effect of recombination rate on the variation of defect density. In this study, the analysis is further to analyze the recombination rate that occurred at the ETL bulk.

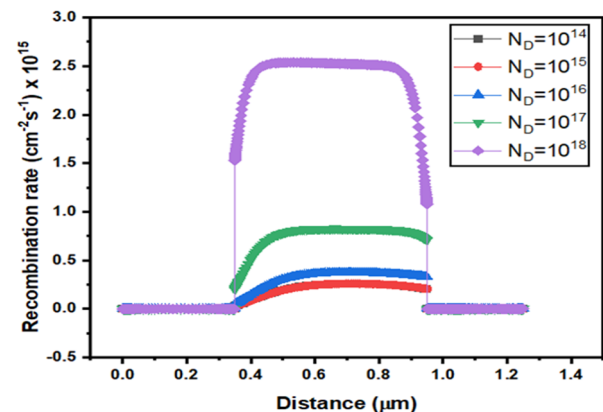


Fig. 6. The recombination rate with the variation of doping density at SnO<sub>2</sub> bulk.

A noticeable change is shown as the doping density increases and the recombination rate decreases (Fig. 6). Specifically, ETLs in PSCs gather and transport charge carriers after the perovskite active layer injects electrons, more critically, ensuring effective charge separation and minimizing charge carrier recombination. An inefficient charge transport could damage the ETL/perovskite interface, which could lead to inhomogeneous charge accumulation and significant interfacial recombination [25], [26]. This means that high-quality ETLs must be designed and fabricated to provide efficient charge conduction and, consequently excellent photovoltaic performance.

### Analysis of the variation of defect at the interface

Only one sort of defect density interface is analyzed, which is neutral. One faulty interface layer proposed is the defect at the interface between the SnO<sub>2</sub> and CH<sub>3</sub>NH<sub>3</sub>PbI<sub>3</sub> layers. The total density of the interface defect was determined to be in the range of 10<sup>10</sup> cm<sup>-2</sup> to 10<sup>16</sup> cm<sup>-2</sup>. When the defect density increased in the solar cell, efficiency decreased (Fig. 7). The performance of the PSC increased as a result of reduced carrier loss owing to recombination as a result of low defect density. Higher defect densities, on the other hand, lead to shorter diffusion lengths, which promotes charge carrier recombination [27]. Consequently, there is a considerable decline in PSC performance.

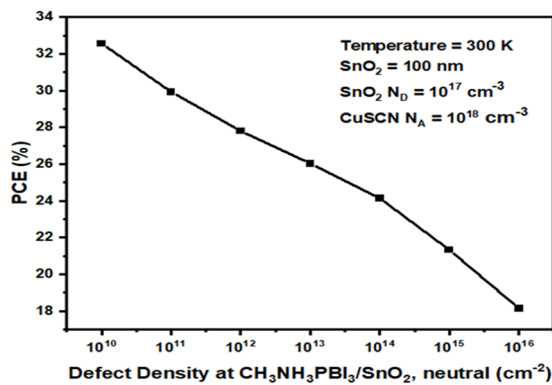


Fig. 7. The variation of defect density at CH<sub>3</sub>NH<sub>3</sub>PbI<sub>3</sub>/SnO<sub>2</sub>

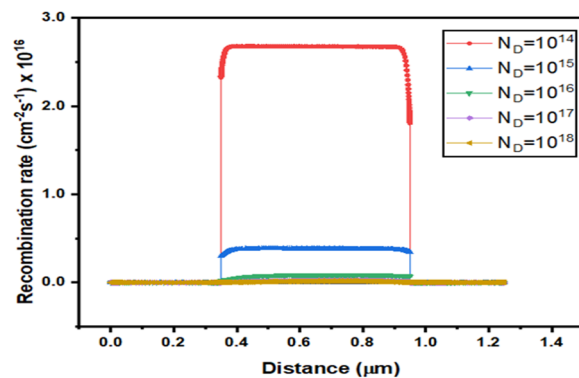


Fig. 8. The recombination rate with the variation of defect density at CH<sub>3</sub>NH<sub>3</sub>PbI<sub>3</sub>/SnO<sub>2</sub>

Next, the recombination rate at the interface of CH<sub>3</sub>NH<sub>3</sub>PbI<sub>3</sub>/SnO<sub>2</sub>. This is performed by changing the defect density value at the interface with a variation range of 10<sup>14</sup> cm<sup>-2</sup> to 10<sup>18</sup> cm<sup>-2</sup>. This investigation is then carried out to investigate further the impact of defect density at the tin oxide-perovskite interface. The open-circuit losses in the PSCs are caused mainly by the recombination that occurs in the bulk layer of the Perovskite and at either the perovskite transport layer interfaces or the transport layer

[25]. Theoretically, the defect density is correlated with the recombination rate, which causes the solar cell efficiency to fall. This is the first-ever study reported on the recombination rate for defect density at CH<sub>3</sub>NH<sub>3</sub>PbI<sub>3</sub>/SnO<sub>2</sub>. As shown in the figure, the recombination rate decrease as the defect density increases (Fig. 8). The result of this recombination rate is classified as a special instance that will be explored further because it is not a common occurrence.

### Analysis of the variation based on optimum value for all parameters

The optimum values for all parameters achieved from the simulation analysis are listed in the table. The simulation findings demonstrate that SnO<sub>2</sub> produced the optimized efficiency by replacing all parameters with the optimal value. The PCE achieved is 24.14%, which is higher than the previous study conducted by Raoui and his team [14] where the highest PCE obtained is below 20%. This demonstrates the need to optimize the ETL layer parameter to attain a higher PCE. Figure 9 displays the optimized PSC structure's J-V curve using SnO<sub>2</sub> as an ETL. FF of 85.99%, V<sub>OC</sub> of 1.15V, and J<sub>SC</sub> of 24.42 mA/cm<sup>2</sup> resulted in a PCE of 24.14%.

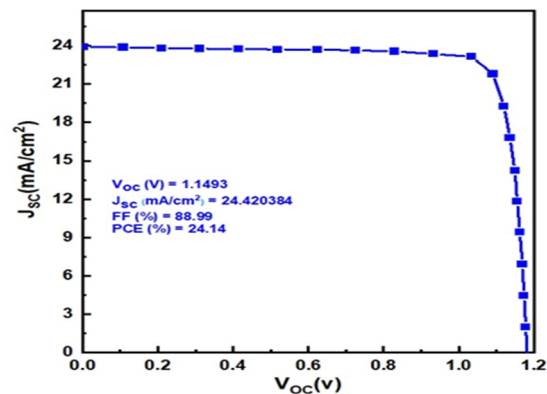


Fig 9. The optimized PSC structure's J-V curve

Table 2. Optimum parameters for SnO<sub>2</sub> as ETL in inorganic perovskite solar cell based on computational analysis.

Parameter	SnO <sub>2</sub>
Layer thickness, d (μm)	100
Bandgap energy, E <sub>g</sub> (eV)	3.6
Electron affinity (eV)	4
Dielectric permittivity, ε (relative)	9
Effective density of conduction band, N <sub>C</sub> (cm <sup>-3</sup> )	2.2 × 10 <sup>18</sup>
Effective density of valence band, N <sub>V</sub> (cm <sup>-3</sup> )	1.8 × 10 <sup>19</sup>
Thermal velocity of electrons, V <sub>e</sub> (cm/s)	100
Thermal velocity of holes, V <sub>h</sub> (cm/s)	25
Electron mobility, μ <sub>e</sub> (cm <sup>2</sup> /Vs)	1 × 10 <sup>7</sup>
Hole mobility, μ <sub>h</sub> (cm <sup>2</sup> /Vs)	1 × 10 <sup>7</sup>
Density of donors, N <sub>D</sub> (cm <sup>-3</sup> )	1 × 10 <sup>17</sup>
Density of acceptors, N <sub>A</sub> (cm <sup>-3</sup> )	NA

### Conclusion

Perovskite solar cell is categorized as the third generation of the solar cell. It consists of 3 main components: the ETL, absorber, and HTL. Various analyses and investigations have been conducted in both simulation and fabrication to improve the efficiency of PSC. SnO<sub>2</sub> is a promising ETL with favorable attributes such as a wide optical band gap (up to 4.0 eV), good transmittance feature, and can be processed by the low-temperature method.

In this study, a PSC structure of ITO/SnO<sub>2</sub>/CH<sub>3</sub>NH<sub>3</sub>PbI<sub>3</sub>/CuSCN has been analyzed by using the SCAPS-1D simulator. The main purpose of this analysis is to design a PSC structure by utilizing SnO<sub>2</sub> as an ETL. The

parameters involved in designing the finest structure include the working temperature of a solar cell, the thickness of ETL, the dopant density of both ETL and HTL, and the defect density at the ETL and absorber interface. The optimum efficiency obtained is 24.14% at 300 K working temperature, 0.10  $\mu\text{m}$  thickness of  $\text{SnO}_2$ ,  $10^{17} \text{ cm}^{-3}$  doping donor density,  $10^{18} \text{ cm}^{-3}$  doping acceptor density, and  $10^{14} \text{ cm}^{-2}$  defect density.

### Acknowledgement

*This work of was supported by Universiti Teknikal Malaysia, Melaka, Malaysia. The work of Farah Liyana Rahim was supported by Universiti Teknikal Malaysia, Melaka.*

### Author

*Farah Liyana Rahim, Universiti Teknikal Malaysia Melaka, Email: farah\_liyana24@yahoo.co; Faiz bin Arith, Universiti Teknikal Malaysia Melaka, Email: faiz.arith@utem.edu.my; Nabilah Ahmad Jalaludin, Universiti Teknikal Malaysia Melaka, Email: nabilahahmad98@gmail.com; Fauziyah Salehuddin, Universiti Teknikal Malaysia Melaka, Email: fauziyah@utem.edu.my; Ahmad Shahiman Mohd Shah, Universiti Malaysia Pahang Al-Sultan Abdullah, Email: asyahiman@ump.edu.my; Ahmad Nizamuddin Mustafa, Universiti Teknikal Malaysia Melaka, Email: nizamuddin@utem.edu.my;*

### REFERENCES

- [1] T. Wu, Z. Qin, Y. Wang, Y. Wu, W. Chen, S. Zhang, M. Cai, S. Dai, J. Zhang, J. Liu, Z. Zhou, X. Liu, H. Segawa, H. Tan, Q. Tang, J. Fang, Y. Li, L. Ding, Z. Ning, Y. Qi, Y. Zhang, and L. Han, "The Main Progress of Perovskite Solar Cells in 2020–2021," *Nano-Micro Lett.*, vol. 13, no. 1, 2021, doi: 10.1007/s40820-021-00672-w.
- [2] B. Osman, T. Abdolkader, and I. Ahmed, "A Review of Perovskite Solar Cells," *Int. J. Mater. Technol. Innov.*, vol. 0, no. 0, pp. 0–0, 2021, doi: 10.21608/ijmti.2021.78369.1032
- [3] N. S. N. M. Alias, F. Arith, A. N. M. Mustafa, M. M. Ismail, S. A. M. Chachuli, and A. S. M. Shah, "Compatibility of Al-doped ZnO electron transport layer with various HTLs and absorbers in perovskite solar cells," *Appl. Opt.*, vol. 61, no. 15, p. 4535, 2022.
- [4] N. S. Nooraid, F. Arith, A. N. Mustafa, P. Chelvanathan, M. I. Hossain, M. A. Azam and N. Amin, "Improved performance of lead-free Perovskite solar cell incorporated with TiO<sub>2</sub> ETL and CuI HTL using SCAPS," *Appl. Phys. A Mater. Sci. Process.*, vol. 129, no. 2, pp. 1–16, 2023
- [5] Y. Ammaih and B. Hartiti, "Optimization of Parameters for Deposition of SnO<sub>2</sub> Films by Sol-Gel using Taguchi Method," no. li, pp. 2–5, 2015
- [6] H. A. Aribisala, "Improving the Efficiency of Solar Photovoltaic Power System," 2013.
- [7] R. Kent, "Renewables," *Plast. Eng.*, vol. 74, no. 9, pp. 56–57, 2018, doi: 10.1002/peng.20026
- [8] M. A. Green, "Third generation photovoltaics: Solar cells for 2020 and beyond," *Phys. E Low-Dimensional Syst. Nanostructures*, vol. 14, no. 1–2, pp. 65–70, 2002, doi: 10.1016/S1386-9477(02)00361-2.
- [9] P. Zhang, J. Wu, T. Zhang, Y. Wang, D. Liu, H. Chen, L. Ji, C. Liu, W. Ahmad, Z. D. Chen, and S. Li, "Perovskite Solar Cells with ZnO Electron-Transporting Materials," *Adv. Mater.*, vol. 30, no. 3, pp. 1–20, 2018, doi: 10.1002/adma.201703737.
- [10] O. V. Aliyaselvam, F. Arith, A. N. Mustafa, P. Chelvanathan, M. A. Azam and N. Amin. Incorporation of green solvent for low thermal budget flower-like Copper(I) Iodide ( $\gamma$ -CuI) for high-efficiency solar cell. *J Mater Sci: Mater Electron* 34, 1274, 2023.
- [11] Q. Jiang, X. Zhang, and J. You, "SnO<sub>2</sub>: A Wonderful Electron Transport Layer for Perovskite Solar Cells," *Small*, vol. 14, no. 31, pp. 1–14, 2018, doi: 10.1002/smll.201801154.
- [12] M. Łuszczek, "Simulation investigation of perovskite-based solar cells," *Electrotech. Rev.*, vol. 1, no. 5, pp. 101–104, 2021, doi: 10.15199/48.2021.05.17.
- [13] P. Zhao, Z. Lin, J. Wang, M. Yue, J. Su, J. Zhang, J. Chang, and Y. Hao, "Numerical Simulation of Planar Heterojunction Perovskite Solar Cells Based on SnO<sub>2</sub> Electron Transport Layer," *ACS Appl. Energy Mater.*, vol. 2, no. 6, pp. 4504–4512, 2019, doi: 10.1021/acsaem.9b00755.
- [14] Y. Raoui, H. Ez-Zahraoui, N. Tahiri, O. El Bounagui, S. Ahmad, and S. Kazim, "Performance analysis of MAPbI<sub>3</sub> based perovskite solar cells employing diverse charge selective contacts: Simulation study," *Sol. Energy*, vol. 193, no. October, pp. 948–955, 2019, doi: 10.1016/j.solener.2019.10.009.
- [15] E. Karimi and S. M. B. Ghorashi, "The Effect of SnO<sub>2</sub> and ZnO on the Performance of Perovskite Solar Cells," *J. Electron. Mater.*, vol. 49, no. 1, pp. 364–376, 2020, doi: 10.1007/s11664-019-07804-4.
- [16] O. V. Aliyaselvam, S. A. Mat Junos, F. Arith, N. Izlan, M. M. Said, A. N. Mustafa, "Optimization of Copper (I) Thiocyanate as Hole Transport Material for Solar Cell by Scaps-1D Numerical Analysis," *Przeglad Elektrotechniczny*, vol. 6, pp. 131-135, 2022.
- [17] F. Jahantigh and M. J. Safikhani, "The effect of HTM on the performance of solid-state dye-sanitized solar cells (SDSSCs): a SCAPS-1D simulation study," *Appl. Phys. A Mater. Sci. Process.*, vol. 125, no. 4, pp. 1–7, 2019, doi: 10.1007/s00339-019-2582-0.
- [18] C. Mebarkia, D. Dib, H. Zerfaoui, and R. Belghit, "Energy efficiency of a photovoltaic cell based thin films CZTS by SCAPS," *J. Fundam. Appl. Sci.*, vol. 8, no. 2, p. 363, 2016, doi: 10.4314/jfas.v8i2.13
- [19] D. Dey, D. De, A. Ahmadian, F. Ghaemi, and N. Senu, "Electrically Doped Nanoscale Devices Using First - Principle Approach: A Comprehensive Survey," *Nanoscale Res. Lett.*, 2021, doi: 10.1186/s11671-020-03467-x
- [20] L. Xiong, Y. Guo, J. Wen, H. Liu, G. Yang, P. Qin, and G. Fang, "Review on the Application of SnO<sub>2</sub> in Perovskite Solar Cells," *Adv. Funct. Mater.*, vol. 28, no. 35, 2018, doi: 10.1002/adfm.201802757.
- [21] K. Ojoto, "Simulation of an Optimized Poly 3-Hexylthiophene (P3HT) based solid state Dye Sensitized Solar Cell (ss-DSSC) using SCAPS," vol. 5, no. April, pp. 1–10, 2020.
- [22] M. A. Mustafa, F. Arith, N. S. Nooraid, M. S. I. M. Zin, K. S. Leong, F. A. Ali, A. N. M. Mustafa, and M. M. Ismail. "Towards a Highly Efficient ZnO Based Nanogenerator" *Micromachines* 13, no. 12: 2200, 2022
- [23] N. S. N. M. Alias, F. Arith, A. Mustafa, M. M. Ismail, N. F. Azmi, and M. Saifizi, "Impact of Al on ZnO electron transport layer in perovskite solar cells," *J. Eng. Technol. Sci.* 54, 2022.
- [24] D. Liu, Y. Wang, H. Xu, H. Zheng, T. Zhang, P. Zhang, F. Wang, J. Wu, Z. Wang, Z. Chen, and S. Li "SnO<sub>2</sub> -Based Perovskite Solar Cells: Configuration Design and Performance Improvement," vol. 1800292, pp. 1–22, 2019, doi: 10.1002/solr.201800292
- [25] H. Pan, X. Zhao, X. Gong, H. Li, N. Haji Ladi, X. L. Zhang, W. Huang, S. Ahmad, L. Ding, Y. Shen, M. Wang, and Y. Fu, "Advances in design engineering and merits of electron transporting layers in perovskite solar cells," *Mater. Horizons*, vol. 7, no. 9, pp. 2276–2291, 2020, doi: 10.1039/d0mh00586j
- [26] N. S. Nooraid, F. Arith, A. Y. Firhat, A. N. Mustafa, and A. S. M. Shah, "SCAPS Numerical Analysis of Solid-State Dye-Sensitized Solar Cell Utilizing Copper (I) Iodide as Hole Transport Layer," *Engineering Journal*, vol. 26, no. 2, pp. 1-10, Feb. 2022.
- [27] K. B. Nine, M. F. Hossain, and S. A. Mahmood, "Analysis of Stable, Environment Friendly and Highly Efficient Perovskite Solar Cell," *IEEE Reg. 10 Annu. Int. Conf. Proceedings/TENCON*, vol. 2019-October, pp. 1825–1828, 2019, doi:
- [28] N. S. N. M. Alias, F. Arith, A. N. M. Mustafa, M. A. Azam, S. H. M. Suhaimy, and O. A. Al-ani, "Effect of Low Temperature Annealing on Anatase TiO<sub>2</sub> Layer as Photoanode for Dye-Sensitized Solar Cell," *Przeglad Elektrotechniczny* vol. 97, no. 10, 2021.